PRESSURE ANALYSIS OF A WELL WITH AN INCLINED HYDRAULIC FRACTURE IN A NATURALLY FRACTURED RESERVOIR

A

PROJECT

Presented to the Faculty

of the African University of Science and Technology

in Partial Fulfilment of the Requirements

for the Degree of

MASTER OF SCIENCE IN PETROLEUM ENGINEERING

By

Meredith, Babatunde Oladipo

Abuja, Nigeria

December, 2009

PRESSURE ANALYSIS OF A WELL WITH AN INCLINED HYDRAULIC FRACTURE IN A NATURALLY FRACTURED RESERVOIR

By

Meredith, Babatunde Oladipo

RECOMMENDED: …….....
Chair, Professor Djebbar TIAB

…….....
Professor David OGBE

….....
Professor Ekwerre PETERS

APPROVED: …….....
Chief Academic Officer

…….....
DATE.

DEDICATION

THIS PROJECT IS DEDICATED TO THE LORD GOD ALMIGHTY.

ACKNOWLEDGEMENT

Special thanks to Almighty God for his support and ultimate guidance throughout this project write up. My profound gratitude goes to all the faculty members of AUST-Abuja for their support.

Special appreciation to my 'special girl friends'-Laide,Femi,Jummy,Taiwo,Kehinde,Yemisi and Motunrayo;and my parents,Mr & Mrs Meredith.

I will like to express my sincere gratitude to my wonderful friends who made my stay in thiscampus interesting-Ojo,Elvis,Kunle,Haruna,Harry,Ene,Aminu,Atsu,Dorcas, Femi,Bismark,the Obodos,Ojemba and all the other lovely AUST students.

I will never forget to appreciate Mr. Olajide Babatunde for his brotherly support.

My ultimate gratitude goes to my supervisor Prof D.Tiab, Prof Chukwu and Prof Osisanya for their technical, moral and fatherly supports. I appreciate his assistance and the precious time he used on this work .

I also acknowledge the support and encouragement given by brothers I never had the opportunity of having as biological brothers-Babatunde Kazeem and Mannix Ighodalo for their brotherly care and understanding.

Table of contents

Chapter 3

Chapter 4

Chapter 5

List of Figures

List of Tables

Abstract

Hydraulic fracturing has been an effective technique to stimulate damaged wells or wells producing from low-permeability formation. It has been established that the orientation of a hydraulic fracture is perpendicular to the direction of the least principal stress in the formation. Thus, most pressure transient analysis techniques are based on the assumption that the fracture is vertical. However, it is now generally agreed that the direction of the least principal stress is not always parallel or perpendicular to the plane of the formation. For this reason it is very likely that some hydraulically fractured wells have inclined fractures.

Objectives of study:

(1) Provide background to justify the conclusion that the direction of least principal stress might be at an orientation different from parallel or perpendicular to the bedding plane of the formation.

(2) Develop a technique, based on the pressure derivative concept, for interpreting pressure transient tests in wells with an inclined hydraulic fracture. Three cases are possible:

(a) the fracture is symmetric in both lateral and horizontal directions,

(b) the fracture is asymmetric in only one of the directions, and

(c) The fracture is asymmetric in both directions.

CHAPTER 1
INTRODUCTION

1.1 Introduction

Hydraulic fracturing is an important well stimulation technique that has been widely used in the oil and gas industry. The technique involves creation of fractures or fracture system in porous medium to overcome wellbore damage, to improve oil and gas productivity in low permeability reservoirs or to increase production in secondary recovery operations. Most of the pressure transient analysis techniques used to analyze pressure responses of fractured wells are based on the assumption that the fracture is either vertical or horizontal. However, hydraulic fracture could be inclined with a certain angle with respect to the vertical direction because it is now generally agreed that the direction of the least principal stress is not always parallel or perpendicular to the plane of the formation. For this reason it is very likely that some hydraulically fractured wells have inclined fractures. This has been proved by laboratory experiments as well as data from actual field studies with the aid of modern technology such as surface tilt meters. Thus, for an inclined hydraulic fracture, the vertical orientation assumption may lead to serious errors in well test analysis especially when the inclination angle is high. More so, there are very few studies concerning pressure transient analysis of inclined hydraulic fracture and there is not any applicable well test analysis procedure available for inclined fractures. For this reason, it is important to develop well test analysis procedures for this type of fracture in naturally fractured reservoirs.

A naturally fractured reservoir can be defined as a reservoir that contains fractures (planar discontinuities) created by natural processes like diastrophism and volume shrinkage, distributed as a consistent connected network throughout the reservoir. They present unique challenges that differentiate them from conventional reservoirs. It represents over 20% of the world's oil and gas reserves, but is however among the most complicated class of reservoirs to characterize and produce efficiently.

The purpose of this study is to develop a technique, based on the pressure derivative concept, for interpreting pressure transient tests in wells with an inclined hydraulic fracture in a naturally fractured reservoir. This report will provide some background on inclined hydraulic fracture including in-situ stress state, factors that affect the stress state, occurrences of inclined hydraulic fractures and field studies. Two techniques of transient pressure analysis using pressure derivatives will be developed. They are type curve matching and Tiab's Direct Synthesis (TDS). Both uniform flux and infinite conductivity models would be considered in the study. Analytical solution for each flow regime will be analysed in details.

1.2 Technical Objectives:

- To provide background to justify the conclusion that the direction of least principal stress might be at an orientation different from parallel or perpendicular to the bedding plane of the formation.
- To develop a technique, based on the pressure derivative concept, for interpreting pressure transient tests in wells with an inclined hydraulic fracture in naturally fractured reservoirs.

Three cases are possible:

(a) The fracture is symmetric in both lateral and horizontal directions,

(b) The fracture is asymmetric in only one of the directions, and

(c) The fracture is asymmetric in both directions.

1.3 Hydraulically fractured wells

Naturally fractured reservoirs are different from conventional (unfractured) reservoirs. They are heterogeneous in type and consist of matrix blocks separated from one another by the fracture system. The matrix blocks are made of the original rock that was present before fracturing took place. The matrix is characterized by its permeability km and porosity φ_m . The fracture system is characterized by its permeability k_f and porosity φ_f . It means a naturally fractured reservoir is a double-porosity and double-permeability reservoir.

1.4 Naturally Fractured Reservoirs

Fractures are displacement discontinuities in rocks, which appear as local breaks in the natural sequence of the rock's properties.It may appear as micro-fissures with an extension of only several micrometers, or as continental fractures with an extension of several thousand kilometres.

In geological terms, a fracture is any planar or curvi-planar discontinuity that has formed as a result of a process of brittle deformation in the earth's crust.Naturally fractured rocks can be geologically categorized into three main types, based on their porosity systems:

(1) Intercrystalline-intergranular;

(2) Fracture-matrix ; and

(3) Vugular-solution

There are four types of naturally fractured reservoirs, based on the extent to which fractures have altered the porosity and permeability of the reservoir matrix:

Type 1: In type 1 reservoirs, fractures provide all the reservoir storage capacity and permeability.

Type 2: In type 2 reservoirs, the matrix already has very good permeability. The fractures add to the reservoir permeability and can result in considerably high flow rates.

Type 3: In type 3 naturally fractured reservoirs, the matrix has negligible permeability but contains most if not all the hydrocarbons. The fractures provide the essential reservoir permeability.

Type 4: In type 4 reservoirs,the fractures are filled with minerals. These types of fractures tend to form barriers to fluid migration and partition formations into relatively small blocks.

1.5 Indicators of Natural Fractures

Pressure transient analysis in naturally fractured reservoirs has received considerable attention in the petroleum literature. Warren and Root assumed that the formation fluid flows from the matrix to fractures under pseudosteady state and showed that a semi-log pressure buildup curve similar to that shown in Figure1.1 is typical of a fractured formation. If the existing fractures dominantly trend in a single direction, the reservoir may appear to have anisotropic permeability.

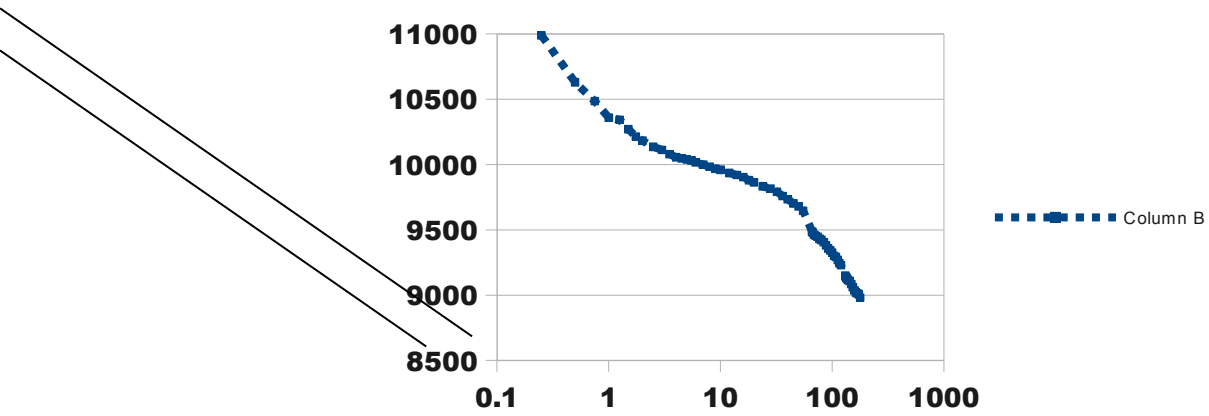

Figure 1.1 Pressure build-up curve from a naturally fractured reservoir.

1.6 Identification of Natural Fractures

It is essential to identify fractures during exploration and drilling. Well logs are useful tools in identifying these natural fractures. A program for fracture detection based on logging techniques consists of using different logs:

- Borehole televiewer logs can be used to identify induced and natural fractures.
- Acoustic, receptivity, and temperature logs can be used to obtain a realistic picture of fractures and their width and orientation in the vicinity of wellbore.
- Variable-density logs can define fracture intervals.

Both core analysis and logging are valuable techniques for explored wells in detecting fracture

porosity φ_f , permeability k_f ,and nature of the matrix or inter-granular porosity. However, there are many wells drilled where no core was taken and the logs do not show any evidence of fractures. Therefore,well test analysis is the only technique used for getting information about the fractured nature of formation, and can provide information on fractured reservoir parameters, size and shape of the matrix blocks, and the nature and orientation of the fracture pattern, in addition to determining P or Pi and skin factor s.

CHAPTER 2
LITERATURE REVIEW

2.1 Practical Well Test Analysis Methods for Hydraulically Fractured Wells in Dual-Porosity Reservoirs.

Many oil and gas fields produce from reservoirs which contain natural fractures that contribute to production. Reservoirs of this type have been found to exhibit, a characteristic pressure transient behavior and are commonly referred as naturally fractured reservoirs. Many methods have been presented for analyzing pressure transient data from naturally fractured reservoirs to estimate reservoir properties. Gringarten and Ersaghi and Aflaki have presented summaries of analysis methods for naturally fractured reservoir well tests (Lancaste,1986).

Many naturally fractured reservoirs have sufficient permeability to produce at economic flow rates without requiring stimulation. However, some naturally fractured reservoirs, such as the Eastern Devonian Gas Shales, have low effective permeability and require some type of stimulation to achieve commercial production rates. A commonly-applied stimulation method is to create a conductive hydraulic fracture in the reservoir by pumping fluid and proppant into the formation at high pressures. When successful, these hydraulic fractures can substantially improve the performance of low-permeability reservoirs.

To optimize the design and implementation of fracture stimulation treatments, it is often desirable to determine the effective propped length and conductivity of the hydraulic fracture following the treatment. Pressure transient testing has been found to produce characteristic data which can be analysed to estimate the effective hydraulic fracture properties. Many methods have been presented for analyzing these data from hydraulically fractured wells in a conventional reservoir. Unfortunately, little information is available to help the engineer analyse pressure transient data for a well completed in a dual-porosity reservoir which has been fracture stimulated.

2.2 Estimating the Pressure-Transient Response for a Horizontal or a Hydraulically Fractured Well at an Arbitrary Orientation in an Anisotropic Reservoir

Tectonic stresses control the direction of growth of both natural fracture systems and hydraulic fractures. If the tectonic stresses have changed since the formation of the natural fracture system, the hydraulic fracture may have a different orientation from the natural fractures. This may even

occur because of production. Cases have been documented where repeat fracture treatments had a different orientation from the original fractures because of the change in the tectonic stresses caused by reservoir depletion (J.P Spivey, Holditch,1999).

To the best of our knowledge, the fractured well case has been studied only for the situation where the hydraulic fracture is parallel to one of the principal axes of permeability.

We present new analytical solutions for these two situations. The new solutions are obtained by transforming the original problem with anisotropic permeability into an equivalent problem with isotropic permeability. Thus, the pressure transient response in an anisotropic system cannot be distinguished from that of an isotropic system from the shape of the pressure response alone. The major contribution of this article is to define the properties of the equivalent isotropic system in terms of the properties of the original anisotropic system. Any existing solution for an isotropic system can then be used to evaluate the pressure response.

For the hydraulically fractured well case, we assume a finite-conductivity fracture. The infinite-conductivity fracture case may be obtained in the limit as the fracture conductivity increases.

2.3 The Evolution of the State of the Art in Well Test Analysis.

Well test analysis has been used for many years to assess well condition and obtain reservoir parameters. Early interpretation methods (by use of straight lines or log-log pressure plots) were limited to the estimation of well performance. With the introduction of pressure-derivative analysis in 1983 and the development of complex interpretation models that are able to account for detailed geological features, well test analysis has become a very powerful tool for reservoir characterization. A new milestone has been reached recently with the introduction of deconvolution. Deconvolution is a process that converts pressure data at variable rate into a single drawdown at constant rate, thus making more data available for interpretation than in the original data set, in which only periods at constant rate can be analyzed. Consequently, it is possible to see boundaries in deconvolved data, a considerable advantage compared with conventional analysis, in which boundaries often are not seen and must be inferred. This has a significant impact on the ability to certify reserves(Alain C. Gringarten,2008).

Results that can be obtained from well testing are a function of the range and the quality of the pressure and rate data available and of the approach used for their analysis. Consequently, at any given time, the extent and quality of an analysis (and therefore what can be expected from well test interpretation) are limited by the state-of-the-art techniques in both data acquisition and analysis. As

data improve and better interpretation methods are developed, more and more useful information can be extracted from well test data.

Early well test analysis techniques were developed independently from one another and often gave widely different results for the same tests (Ramey 1992). This has had several consequences:

• An analysis was never complete because there always was an alternative analysis method that had not been tried.

• Interpreters had no basis on which to agree on analysis results.

• The general opinion was that well testing was useless given the wide range of possible results.

Significant progress was achieved in the late 1970s and early 1980s with the development of an integrated methodology on the basis of signal theory and the subsequent introduction of derivatives. It was found that, although reservoirs are all different in terms of depth, pressure, fluid composition, geology, etc., their behaviors in well tests were made of a few basic components that were always the same. Well test analysis was about finding these components, which could be achieved in a systematic way, following a well-defined process. The outcome was a well test interpretation model, which defined how much and what kind of knowledge could be extracted from the data. The interpretation model also determined which of the various published analysis methods were applicable and when they were applicable. Importantly, the integrated methodology made well test analysis repeatable and easy to learn. The evolution of the state-of-the-art techniques in well test analysis throughout these years can be followed from review papers that have appeared at regular intervals in the petroleum literature (Ramey 1980, 1982, 1992; Gringarten 1986; Ehlig-Economides et al. 1990).

2.4 Transient Pressure Behaviour of Naturally Fractured Reservoirs

The naturally fractured reservoir model presented by Warren and Root was extended to improve analysis of field data and to account for practical wellbore and reservoir conditions. These conditions include wellbore storage and damage, and constant producing pressure in infinite define pseudo-steady state and pressure in infinite define pseudo-steady state and long time reservoir behaviour.

In recent years, numerous models have been proposed to explain transient pressure behavior of naturally fractured reservoirs. The term "naturally fractured" can be misleading. In reality, these models consider a reservoir composed of two porous media regions, primary and secondary porosity. Primary porosity is primary and secondary porosity. Primary porosity is synonymous with

the matrix rock whose properties are controlled by sedimentation, cementation, and lithification of the original deposits. Secondary porosity, i.e., the fracture network, is considered to porosity, i.e., the fracture network, is considered to have been developed subsequent to the primary system as a result of mechanical deformation, solution, or dolimitization of the original matrix.

Streltsova presented a thorough discussion of fluid flow in fractured reservoirs and included the classification system illustrated in Figure 1. Four media categories are utilized as follows. The first, a fractured medium, consists of a formation whose primary porosity contains the majority of the fluid primary porosity contains the majority of the fluid storage volume while the secondary porosity contributes the transmissivity of the zone. This is the situation most frequently modeled to describe naturally fractured reservoir pressure. A purely fractured medium was envisioned as a system whose matrix permeability and porosity were negligible. In this case, the storativity and transmissivity of the reservoir would be due entirely to the fracture network. This classification is one limiting form of the first category behavior. The third group is a double porosity medium in which the storage volumes of the primary and secondary regions are of the same order of magnitude while the transmissivity is a result of the fracture system. The final classification is a heterogeneous medium. In this case, the fracture system is filled with a material of lower permeability than the matrix.

This study concentrates on the first two categories, fractured and purely fractured media. Both treat the reservoir as a continuum. The smallest incremental volume which is visualized mathematically is of an extent large enough to include both primary and secondary porosity. The degree of fracturing is such that the fractures appear to be homogeneously distributed throughout the matrix.

Warren and Root's version of a naturally fractured reservoir model was chosen as the basis for this work for several reasons. The primary reason for this work many publications have been presented which support the analytic results of Warren and Root even with varying idealizations. The model has been applied to interpretation of field data with apparent success, indicating the model's practicality. From an engineering standpoint, these conditions are a necessity.

The study is discussed in four section; Mathematical Development and Idealizations, Limiting Forms of Reservoir Behaviour, Infinite Reservoirs, and Closed Reservoirs, Conclusions from these sections are presented at the end of the paper. presented at the end of the paper. Mathematical Development and Idealizations

In order to develop equations which describe fluid flow in naturally fractured reservoirs, idealizations are necessary to obtain a model in a mathematically tractable form. This section

discusses these idealizations and the method of solution of the governing equations.

This study considers a horizontal radial reservoir initially at uniform pressure with impermeable upper and lower boundaries. The system was treated as a continuum with the fracture network superimposed on the primary porosity. This idealization resulted in two pressures, matrix and fracture, at each location in space.

In naturally fractured reservoirs, the unique pressure behavior due to the double porosity medium and their interaction has lead to the development of a variety of sophisticated models. These models differ from each other in a way the matrix/fracture fluid transfer is handled. The aim of these models is to evaluate the special flow characteristic and provide useful information from interpretation of pressure data.

One of the earliest models was developed by Pollard to quantify skin resistance from pressure buildups and used to evaluate acid treatment in fractured limestone. Not only the skin, but also the fracture and matrix pore volume could be determined from the graphical analysis. The pressure differential in the well was assumed to be in response to three distinct flow regions connected in series. The first region is the damaged or improved region in the fracture near the well (skin region). The second region considers the pressure loss due to the flow resistance within the fractures, and the last one is the pressure response between the matrix and the fracture system. The flux between the matrix and fractures and between fractures and wellbore was assumed to be under pseudosteady state condition.

2.5 Estimation of Average Reservoir Pressure and Drainage Area in Naturally Fractured Reservoirs—Tiab's Direct Synthesis

The behaviour of naturally fractured reservoirs (NFR) at pseudo-steady state is similar to that of a homogeneous reservoir. However,because of the double porosity nature of NFR,the transient behaviour is quiet different. Moreover, it is very important to take matrix flow model into account in estimating the drainage area and average reservoir pressure. The foundations of the various mathematical models that have been developed to describe the flow in double porosity system were laid by Barentblant and Warren and Root. Warren and Root model assumed a matrix cubic model with three orthogonal faces. Furthermore a pseudo-steady state matrix flow into the fracture was assumed. Solutions were obtained for both finite and infinite system. Other authors such as Kazemi and de-Swaan presented mathematical model for matrix transient flow. Mostly slab model has been used extensively in double porosity well test analysis exhibiting matrix transient flow. In 1983 P. A. Witherspoon et al compared the matrix outflow by using slab and cubic model. The result shows that both models gave the same matrix outflow. However, Witherspoon and et al only developed

solution for spherical model. The solution compared with the Warren and Root model shows some differences in the fracture-matrix transition flow. The results for early flow and late time flow were the same. de-Swaan6 made use of various dimensions of rectangular parallel ipipes to model matrix out flow, but his results were never coupled with the fracture flow for well test analysis.

Several methods of well test analysis have been presented. These can be classified into two main categories; conventional method (Horner plot and type curve matching) and TDS technique. The TDS technique makes use of log-log plot of pressure and log derivative data to evaluate reservoir properties without type curve matching or Horner plot. The TDS technique has been applied to both homogeneous and non-homogeneous reservoirs (NFR) in several areas of application. Relevant to this study are; Analysis of pressure and pressure derivative without type-curve matching in vertically fractured wells in closed systems7, Analysis of pressure and pressure derivative without type-curve matching in naturally fractured reservoirs and Analysis of pressure and pressure derivative without type-curve matching in horizontal well tests in naturally fractured reservoirs9. As an extension of the TDS technique, this study presents the evaluation of various models used in well test analysis for the estimation of average reservoir pressure and drainage area in NFR under reservoir pseudo-steady state flow regime. The cubic flow model for the Warren and Root sugar cube model was developed. The results were compared with the Warren and Root pseudo-steady state model using various storativity ratio and matrix inter-porosity flow parameter.

CHAPTER 3
TRANSIENT PRESSURE ANALYSIS OF A WELL WITH AN INCLINED HYDRAULIC FRACTURE IN A NATURALLY FRACTURED RESERVOIR

3.1 Pressure Analysis Of a Well with an Inclined Hydraulic Fracture

3.1.1 Uniform Flux Fracture Model

In this model,a well with an inclined hydraulic fracture is characterised by a fracture linear flow regime followed by an early radial flow regime and then the late time pseudo radial flow regime(Anh &Tiab,2009).

(I) Fracture Linear Flow Regime

At early time when t_D is small enough, linear flow regime is observed and characterized by one half slope line on pressure and pressure derivative plots.

$$\Delta P = \left[\frac{4.064qB}{h}\frac{\left(\cos\theta_w\right)}{y_f}\sqrt{\left(\frac{\mu}{\varphi}c_t k\right)}\right]t^{(1/2)} \tag{3.1}$$

This indicates that a plot of ΔP versus $t^{1/2}$ will yield a straight line with a slope:

$$m_{LF} = \frac{4.064qB}{h}\frac{\left(\cos\theta_w\right)}{y_f}\sqrt{\left(\frac{\mu}{\varphi}c_t k\right)} \tag{3.2}$$

Eq.(3.2) can be used to calculate $\frac{y_f}{\left(\cos\theta_w\right)}$ knowing k or vice versa from the slope m_{LF}

(II) Early Radial Flow Regime

The early radial flow regime for uniform flux model can be identified by a horizontal line on

pressure derivative function plot (tD*P'D vs. tD) with the relationship :

$$(tX\Delta P')_{ER}=\frac{(70.6quB\,X\cos\theta_w)}{kh} \tag{3.3}$$

Eq 3.3 can be used to calculate either k or $\cos(\theta_w)$ knowing the other value.

The relationship between ΔP and t during early radial flow period can be derived from Eq (3.3):

$$(\Delta P)_{ER}=\frac{(70.6quB\,X\cos\theta_w)}{kh}\ln t+C_1 \tag{3.4}$$

Eq (3.4) indicates that a semi-log plot of ΔP vs. t will yield a straight line with slope m_{ER} during early radial flow period:

$$m_{ER}=\frac{(162.56quB\,X\cos\theta_w)}{kh} \tag{3.5}$$

Eq (3.5) can also be used to calculate either k or $\cos(\theta_w)$ knowing either value.

(III) Late Time Pseudo-Radial Flow Regime

The pseudo- radial flow regime can be identified by a horizontal line on pressure derivative function plot (t_D*P'$_D$ vs. t_D) with t_D*P'$_D$ = 0.5.

$$(tX\Delta P')_{PR}=\frac{70.6quB}{kh} \tag{3.6}$$

where (k) can be calculated directly from Eq (3.6)

The relationship between ΔP and t during early radial flow period can be derived from Eq.(3.6):

$$(\Delta P)_{ER}=\frac{(70.6quB)}{kh}\ln t+C_2 \tag{3.7}$$

Eq.(5.48) indicates that a semi-log plot of ΔP vs. t will yield a straight line with slope m_{PR} during

pseudo-radial flow period:

$$m_{PR}=\frac{162.56quB}{kh} \tag{3.8}$$

which can also be used to calculate k.

3.1.2 Infinite Conductivity Fracture Model

The following flow regimes could be observed for a well intersecting an infinite conductivity inclined fracture plane(Anh &Tiab,2009):

(I) Fracture Linear Flow Regime

(II) Bi-radial Flow Regime

(III) Early Radial Flow Regime

(IV) Late Time Pseudo-Radial Flow Regime

(I) Fracture Linear Flow Regime

The linear flow regime for infinite conductivity fracture is the same for uniform flux fracture. Thus, both Eq.(3.1) and (3.2) can be applied for infinite conductivity fracture case.

(II) Bi-radial Flow Regime

This flow regime for vertical infinite conductivity fracture can be recognized by a straight line of slope 0.36 on (t_D*P'$_D$ vs. t_D). The equation for this straight line is

$$(tx\Delta P')=\frac{3.34343quB}{kh}\frac{(\cos\theta_w)}{y_f^{0.72}}\left[\frac{kt}{(\varphi\mu c_t)}\right]^{0.36} \tag{3.9}$$

Eq (3.9) can be used to calculate $\frac{y_f^{0.72}}{(\cos\theta_w)}$ knowing k or vice versa from any point on the bi-radial flow line of (t*ΔP' vs. t) plot.

Eq.(3.9) indicates that a plot of t*ΔP' versus $t^{0.36}$ will yield a straight line with a slope:

$$m_{BR}=\frac{3.34343\text{quB}}{kh}\frac{\left(\cos\theta_w\right)}{y_f^{0.72}}\left[\frac{k}{\left(\varphi\mu c_t\right)}\right]^{0.36} \tag{3.10}$$

Eq.(3.10) can also be used to calculate $\frac{\left(\cos\theta_w\right)}{y_f^{0.72}}$ knowing k or vice versa from m_{BR}

(III) Early Radial Flow Regime

The early radial flow regime for infinite conductivity model can be identified by a horizontal line on pressure derivative function plot ($t_D*P'_D$ vs. t_D) with the relationship presented by:

$$\left(tX\Delta P'\right)_{ER}=\frac{\left(70.6\text{quB}\,X\cos\theta_w\right)^{0.68}}{kh} \tag{3.11}$$

Eq.(3.11) can be used to calculate either k or $\cos(\theta_w)$ knowing the other value. The relationship between ΔP and t during early radial flow period can be derived from Eq.(3.11):

$$\left(\Delta P\right)_{ER}=\frac{\left(70.6\text{quB}\,X\left(\cos\theta_w\right)^{0.68}\right)}{kh}\ln t+C_1 \tag{3.12}$$

Where C_1 is a constant.

Eq.(3.12) indicates that a semi-log plot of ΔP vs. t will yield a straight line with slope m_{ER} during early radial flow period:

$$m_{ER}=\frac{\left(162.56\text{quB}\,X\left(\cos\theta_w\right)^{0.68}\right)}{kh} \tag{3.13}$$

Eq.(3.13) can also be used to calculate either k or $\cos(\theta_w)$ knowing the other value.

(IV) Late Time Pseudo-Radial Flow Regime

The late time pseudo-radial flow regime for infinite conductivity fracture is similar to that of uniform flux fracture.

3.2 TDS Procedure for pressure analysis of a well with an inclined hydraulic fracture

TDS is a powerful technique forcomputation of reservoir parameters of a well with an inclined hydraulic fracture directly from log-log plots of pressure and pressure derivative data without using type curve matching.TDS requires graphing of pressure and pressure derivative on a single log-log plot for direct analysis. The fact that the slopes of the straight lines used in TDS technique are known will minimize error due to objective judgements encountered in other methods During early times theflow of fluids is linear and can be identified by a straight line of slope 0.5. The linearflow line is used to calculate the $\frac{(\cos\theta_w)}{y_f}$ ratio. The second straight line, which happens only at high h_D and θw, is early radial flow period and identified by a horizontal straight line with $t_D*P'_D$ equal a constant. This line can be used to calculate the angle θw. Theinfinite acting radial flow regime (pseudo-radial flow) can be identified by a horizontal straight line of $t_D*P'_D = 0.5$. This flow regime is used to calculate permeability. For the infinite-conductivity fracture case, pressure derivative plots reveal another dominant flow regime happened after linear flow period, called the bi-radial flow. This flow regime,which can be identified by a straight line of slope 0.36, can also be used to calculate the half-fracture length and permeability.

Case 1: Uniform Flux Fracture

The following step-by-step procedure is for the ideal case where all the necessary straight lines are well defined (linear flow and late-time radial flow) shown in Fig 3.1.

Step 1 - A plot of well pressure change ΔP and pressure derivative ($t\times \Delta P'$) values versus test time is made. The presence of a straight line of slope 0.5 (linear flow regime) followed by a horizontal straight line (late-time radial flow regime) indicates that the well is intersected by a uniform flux fracture. As mentioned before, a horizontal straight line may occur between the linear and late-time radial flow regimes, indicative of an early radial flow regime.

Step 2 - Read the value of $(t\times \Delta P')_{PR}$ corresponding to the infinite acting late-time radial flow line.

Step 3 - Calculate the permeability from Eq 3.6

Step 4 - Obtain the value of (t× $\Delta P'$) at time t = 1 hr from the linear flow line (extrapolated if necessary), (t x $\Delta P'$)$_{L1}$. If pressure derivative curve is not well defined, obtain (ΔP)$_{L1}$.

Step 5 - Calculate the ratio, $\frac{y_f}{\cos\theta_w}$, from

$$\frac{y_f}{\cos\theta_w}=\frac{2.032qB}{h(t\times\Delta P')_{L1}}\sqrt{\frac{\mu}{\varphi\, c_t k}} \quad . \tag{3.14}$$

If the linear flow line portion of the (t× $\Delta P'$) is too short or too distorted by near wellbore effect and noise, then $\frac{y_f}{\cos\theta_w}$ should be determined from the half-slope line of ΔP , using Eq.:

$$\frac{y_f}{\cos\theta_w}=\frac{4.064qB}{h(\Delta P)_{L1}}\sqrt{\frac{\mu}{\varphi\, c_t k}} \tag{3.15}$$

then use Eq.:

$$(t\times\Delta P')_{L1}=0.5(\Delta P)_{L1} \tag{3.16}$$

to draw the half-slope line of the pressure derivative curve.

Step 6 - Determine the time of intersection of the linear and pseudo-radial flow line from the graph, i.e. t_{LPRi}, using the (t× $\Delta P'$) curve.

Step 7 - Calculate the ratio $\left(\frac{y_f}{\cos\theta_w}\right)^2/k$ from Eq.:

$$\left(\frac{y_f}{\cos\theta_w}\right)^2=\frac{kt_{LPRi}}{1207\,\mu\varphi\, c_t} \quad . \tag{3.17}$$

Then calculate this ratio using k and $\frac{y_f}{\cos\theta_w}$ values obtained in steps 3 and 5, respectively. If the two ratios are approximately equal, then the values of k and $\frac{y_f}{\cos\theta_w}$ are correct. If these ratios are significantly different, shift one or both straight lines, and repeat steps 2 through 7 until the ratios are equal. Generally, the pressure derivative values during the linear flow regime are more likely to be distorted due to mechanical problems, wellbore storage and skin. Consequently, if the pseudo-

radial flow line is well defined, then the linear flow line is probably the one that should be shifted. A shift to the left will decrease the value of $\frac{y_f}{\cos\theta_w}$ and a shift to the right will increase it.

Step 8 – If early radial flow regime is observed, read the value of $(t\times \Delta P')_{ER}$ corresponding to the early radial flow line. If early radial flow regime cannot be identified, go to Step 14.

Step 9 - Calculate the inclination angle (θ_w) from Eq. 3.3

Step 10 - Calculate the half fracture length, y_f, from the ratio $\frac{y_f}{\cos\theta_w}$ calculated in step 7 and the angle (θ_w) calculated in step 9.

Step 11 - Determine the time of intersection of the linear and early radial flow line from the graph, i.e. t_{LERi}, using the $(t\times \Delta P')$ curve.

Step 12 - Calculate the half fracture length, y_f, from Eq.:

$$y_f^2 = \frac{kt_{LERi}}{1207\,\mu\varphi\, c_t} \tag{3.18}$$

Compare the newly calculated y_f with the one calculated in Step 10. If the two values are approximately equal, then the y_f values are correct. If these values are significantly different, shift the early radial flow horizontal line, and repeat steps 8 through 12 until the two values are equal. Shifting the early radial flow line up will decrease the value of y_f (i.e. increase $\cos(\theta_w)$ or decrease θ_w) and shifting it down will increase y_f(i.e. decrease $\cos(\theta_w)$ or increase θ_w).

Step 13 –Estimate t_{SPR} by calculating t_{SPR} from Equations:

$$t_{Dl} = \frac{25}{3} = \frac{0.0002637\; kt_{SPR}}{\varphi\;\mu\; c_t y_f^2} \tag{3.19}$$

and

$$\theta_w = \arctan\left(\sqrt{\frac{1.26576\times 10^{-4}\; kt_{SPR}}{\varphi\;\mu\; c_t h^2}}\right) \tag{3.20}$$

and taking the maximum value of the two. Skip Steps 14-18 and go on to step 19.

Step 14 – Determine from the graph the starting time of the infinite acting pseudo-radial flow line, t_{SPR}, on the pressure derivative curve.

Step 15 - Calculate the angle (θ_w) from Eq. 3.20

Step 16 - Calculate the half fracture length, y_f, from the ratio $\frac{y_f}{\cos\theta_w}$ calculated in step 7 and angle θ_w calculated in step 15.

Step 17 – Check if y_f and θ_w calculated in step 15 and 16 satisfy the condition:

$$\frac{25}{12}\left(\frac{h}{y_f}\tan\theta_w\right)^2 \geq \frac{25}{3} \quad \text{.....(3.21)}$$

If they do, go to Step 19. Otherwise, continue to step 18.

Step 18 – Use t_{SPR} to calculate y_f from Eq.(3.19), and then compute the angle (θ_w) from the ratio $\frac{y_f}{\cos\theta_w}$ calculated in step 7.

Step 19 – Calculate the pseudo-skin factor, S_{UF}, using Eq.:

$$S_{UF} = \frac{kh\ \Delta P(t_{SPR})}{141.2q\ \mu\ B} - \frac{1}{2}\left[\ln\left(\frac{0.0002637\ kt_{SPR}}{\varphi\ \mu\ c_t y_f^2}\right) + 2.80907\right] \quad (3.22)$$

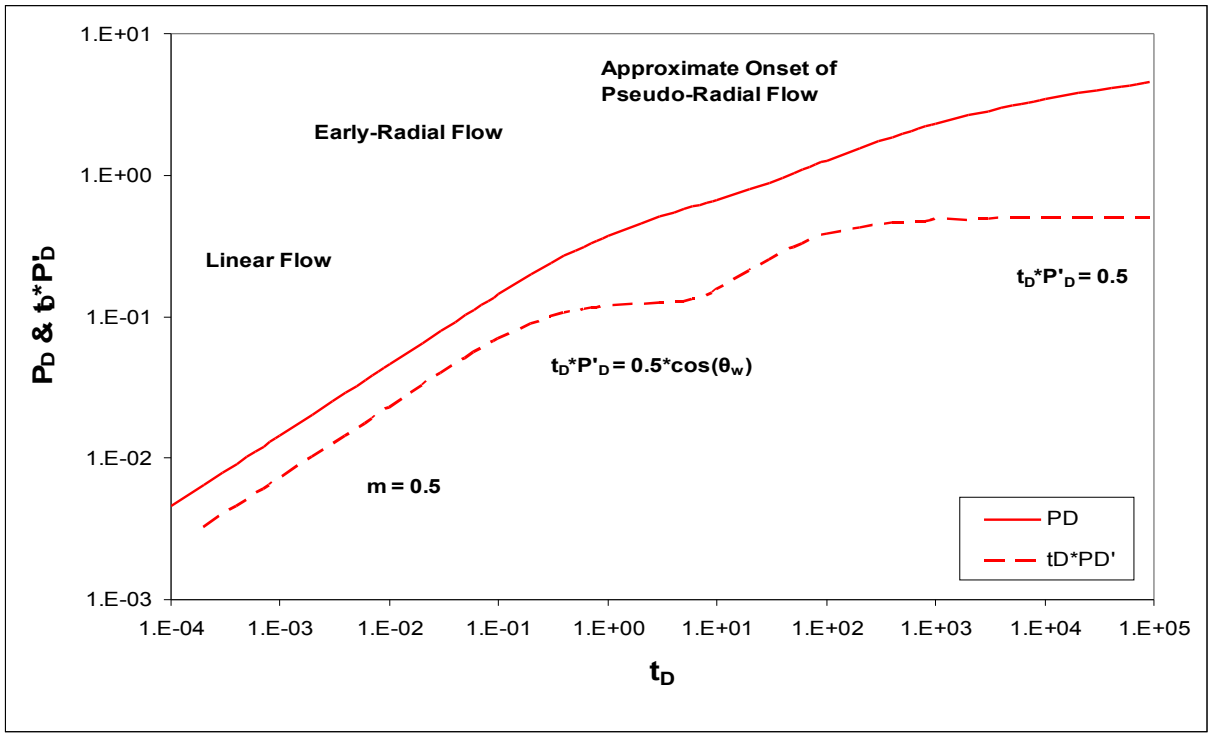

Fig 3.1Pressure & Pressure derivative plots vs time of Uniform flux hydraulic fracture

Case 2: Infinite Conductivity Fracture

If all the necessary straight lines of infinite conductivity inclined fracture (linear,bi-radial and pseudo-radial flow) are well defined as shown in Fig 3.2,the following procedures are recommended:

Step 1 - A plot of well pressure change (ΔP) and pressure derivative (t× $\Delta P'$) values versus test time is made. The presence of a straight line of slope 0.5 (linear flow regime) followed by the bi-radial flow line of slope 0.36 and a horizontal straight line (pseudo-radial flow regime) indicates that the well is intersected by an infinite conductivity fracture. Similar to the uniform flux case, a horizontal straight line may occur between the bi-radial and pseudo-radial flow regimes mentioned above, indicative of an early radial flow regime.

Step 2 - **Step 7** are the same as those in Case 1.

Step 8 - From the bi-radial flow line (extrapolated if necessary) read the value of $(t\times \Delta P')_{BR1}$ at time t = 1 hr.

Step 9 – Calculate the ratio $\frac{y_f^{0.72}}{\cos\theta_w}$ from Eq.:

$$\frac{y_f^{0.72}}{\cos\theta_w}=\frac{3.34343\,q\mu B}{(t\times\Delta P')_{BR1}\,kh}\left(\frac{k}{\varphi\ \mu\ c_t}\right)^{0.36} \tag{3.23}$$

Step 10 – Determine the time of intersection of the bi-radial and pseudo-radial flow line from the graph, i.e. t_{BRPRi}, using the ($t\times \Delta P'$) curve.

Step 11 – Calculate the ratio $\frac{y_f^{0.72}}{\cos\theta_w}$ from Eq.:

$$\frac{y_f^{0.72}}{\cos\theta_w}=0.04736\left(\frac{kt_{BRPRi}}{\varphi\ \mu\ c_t}\right)^{0.36} \tag{3.24}$$

Compare this ratio with the ratio calculated in step 9, if the two ratios are approximately equal, then the value of $\frac{y_f^{0.72}}{\cos\theta_w}$ is correct. If these ratios are significantly different, shift the bi-radial straight lines, and repeat steps 8 through 11 until the ratios are equal.

Step 12 – Calculate y_f and (θ_w) by combining the ratio $\frac{y_f}{\cos\theta_w}$ calculated in step 7 with $\frac{y_f^{0.72}}{\cos\theta_w}$ from step 9.

Step 13 –Estimate t_{SPR} by calculating t_{SPR} from Equation:

$$t_{DI}=25.521=\frac{0.0002637\ kt_{SPR}}{\varphi\ \mu\ c_t y_f^2} \tag{3.25}$$

and

$$t_{DI}=6.3802\frac{h^2}{y_f^2}\left(\tan\theta_w\right)^2=\frac{0.0002637\ kt_{SPR}}{\varphi\ \mu\ c_t y_f^2} \tag{3.26}$$

and taking the maximum value of the two.

Step 14 – Calculate the pseudo-skin factor, S_{IC}, using Eq:

$$S_{IC}=\frac{kh\ \Delta P(t_{SPR})}{141.2\mathrm{q}\ \mu\ B}-\frac{1}{2}\left[\ln\left(\frac{0.0002637\ kt_{SPR}}{\varphi\ \mu\ c_t y_f^2}\right)+2.2\right] \tag{3.27}$$

Early Radial Flow Calculations: If the early radial flow regime is observed, it can be combined with either bi-radial flow or linear flow to find $\cos(\theta_w)$ and y_f. The following steps are recommended:

Step 1.1 – Same as step 8 of Case 1.

Step 1.2 – Calculate the inclination angle (θ_w) from Eq. (3.11)

Step 1.3 – If the linear flow regime is observed, calculate the half fracture length, y_f, from the ratio $\frac{y_f}{\cos\theta_w}$ obtained in step 7 of case 2. If the bi-radial flow regime is observed, y_f can be calculated from the ratio $\frac{y_f^{0.72}}{\cos\theta_w}$ obtained in step 11 of case 2.

Step 1.4 – If the linear flow line is available, determine the time of intersection of the linear and early radial flow line from the graph, i.e. t_{LERi}, using the ($t\times \Delta P'$) curve. If the bi-radial flow line is available, determine the time of the intersection of the bi-radial and early radial flow line from the graph, i.e. t_{BRERi}, using the ($t\times\Delta P'$) curve,.

Step 1.5 - Calculate the half fracture length, y_f, from Eq.:

$$\frac{y_f^2}{(\cos\theta_w)^{0.64}}=\frac{kt_{LERi}}{1207\,\mu\varphi\,c_t} \tag{3.28}$$

for linear flow and Eq.:

$$\frac{y_f^{0.72}}{(\cos\theta_w)^{0.32}}=\frac{1}{21.11}\left(\frac{kt_{BRERi}}{\varphi\,\mu\,c_t}\right)^{0.36} \tag{3.29}$$

for bi-radial flow. Compare the newly calculated y_f with the one calculated in Step 1.3. If the two values are approximately equal, then the y_f values are correct. If these values are significantly different, shift the early radial flow horizontal line, and repeat steps 1.1 through 1.5 until the two values are equal. Shifting the early radial flow line up will decrease the value of y_f (i.e. increase $\cos(\theta_w)$ or decrease θ_w) and shifting it down will increase y_f (i.e. decrease $\cos(\theta_w)$ or increase θ_w).

Starting Time of Pseudo-Radial Flow Calculations: Similar to case 1, the starting time of pseudo-radial flow line can be used to calculate either y_f or θ_w when early radial flow and either linear or bi-radial flow regimes are not available. The calculation steps are as follows:

Step 2.1 – Same as step 14 of case 1.

Step 2.2 – Calculate the angle (θ_w) from Eq.:

$$\theta_w = \arctan\left(\sqrt{\frac{4.1331\times10^{-5}\ kt_{SPR}}{\varphi\ \mu\ c_t h^2}}\right) \qquad (3.30)$$

Step 2.3 - If the linear flow regime is observed, calculate the half fracture length, y_f, from ratio $\frac{y_f}{\cos\theta_w}$ obtained in step 7 of case 2. If the bi-radial flow regime is observed, calculate y_f from the ratio $\frac{y_f^{0.72}}{\cos\theta_w}$ obtained in step 11 of case 2.

Step 2.4 – Check if y_f and θ_w calculated in step 2.2 and 2.4 satisfy the following condition:

$$6.3802\frac{h^2}{y_f^2}\left(\tan\theta_w\right)^2 \geq 25.521 \qquad \text{.....(3.31)}$$

If they do, the following step (2.5) is not necessary. Otherwise, continue to step 2.5.

Step 2.5 – If the linear flow regime is observed, use t_{SPR} to calculate y_f from Eq.(3.25), and then compute the angle (θ_w) from the ratio $\frac{y_f}{\cos\theta_w}$ obtained in step 7 of case 2. If the bi-radial flow regime is observed, calculate the angle (θ_w) from the ratio $\frac{y_f^{0.72}}{\cos\theta_w}$ calculated in step 11 of case 2.

<u>Special Cases:</u>

- *Bi-radial and Pseudo-radial flows are observed. Linear flow is not observed.*

a. Early radial flow is present: For this special case, follow the same steps for case 2 above with following adjustments: Skip steps 4 to 7, replace step 12 with Early radial flow calculations.

b. Early radial flow is not available: skip steps 4 to 7 and replace both step 12 and 13 with Starting time of pseudo radial flow calculations.

- *Linear and Pseudo-radial flows are observed. Bi-radial flow is not observed or not well defined.*

a. Early radial flow is present: skip steps 8 to 11 and replace step 12 with Early radial flow calculations.

b. Early radial flow is not available: skip steps 4 to 7 and replace both step 12 and 13 with Starting time of pseudo radial flow calculations.

Linear and Pseudo-radial flows are observed. Bi-radial flow is not observed or not well defined.

a. Early radial flow is present: skip steps 8 to 11 and replace step 12 with Early radial flow calculations.

b. Early radial flow is not available: skip steps 4 to 7 and replace both step 12 and 13 with Starting time of pseudo radial flow calculations.

- *Linear, Early radial and Bi-radial flows are observed. Pseudo-radial flow is not observed.*

Skip step 2 and 3 and calculate permeability from Eq.:

$$k=\frac{3032.87\,q\mu B\left[\left(t\times\Delta P'\right)_{LI}\right]^{17/8}\left(t_{LBRi}\right)^{17/16}}{h\left[\left(t\times\Delta P'\right)_{ER}\right]^{25/8}} \tag{3.32}$$

Notice that the early radial flow regime must be present in order for this case to work. Checking steps (steps 6, 7, 10 and 11) also need to be skipped. It should be noted that all the results obtained from steps 7 and 11 in case 2 should be replaced by results from steps 5 and 9 respectively for this special case.

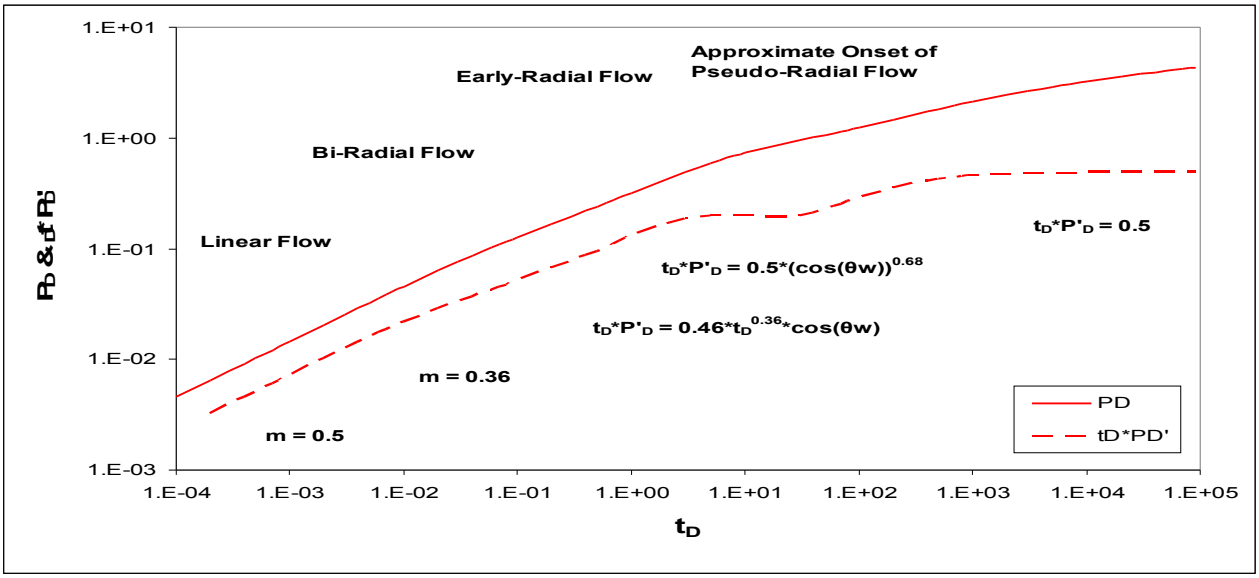

Fig 3.2 *Pressure & Pressure derivative plots vs time of an infinite conductivity hydraulic fracture*

3.3 Estimation of Average Reservoir Pressure in Naturally Fractured Reservoirs

Naturally fractured reservoirs are complex. The density of the fracture network can vary with position in the reservoir, as a function of the rock stresses due to curvature of the formation. When a well is opened in a naturally fractured reservoir, a rapid pressure response occurs in the fissure network due to its high diffusivity. A pressure difference is created between matrix and

fissure, and the matrix blocks start to produce into the fissures. The pressure of the matrix blocks P_m decreases as flow progresses and, finally, tends to equalize with the pressure of the surrounding fissures P_t.

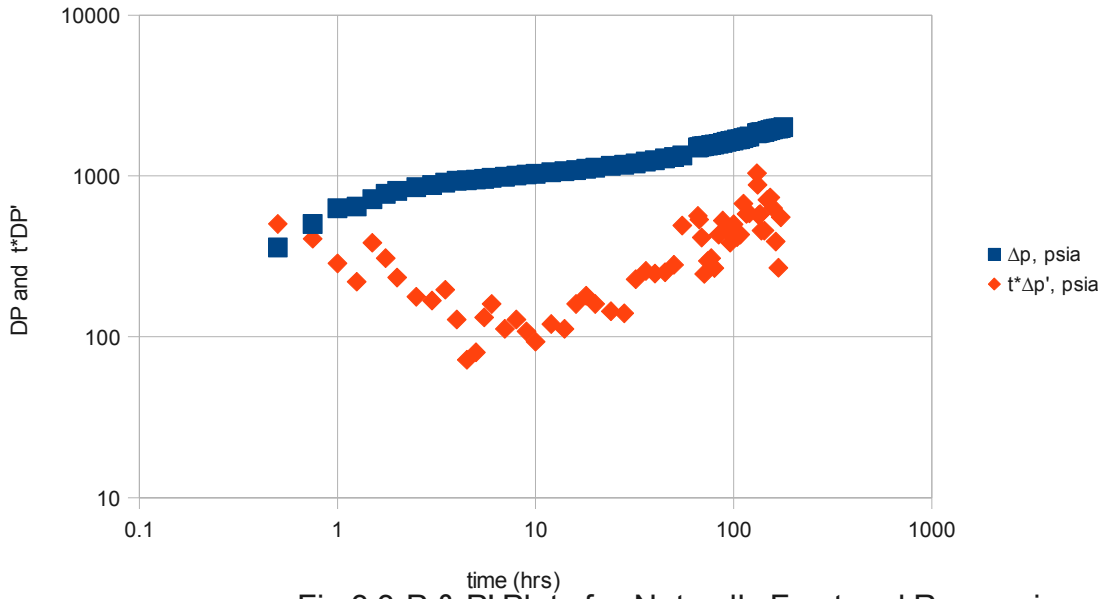

Fig 3.3 P & P' Plot of a Naturally Fractured Reservoir

The behaviour of naturally fractured reservoirs (NFR) at pseudo-steady state is similar to that of a homogeneous reservoir. However, because of the double porosity nature of NFR, the transient behaviour is quiet different.

The procedure for the application of the TDS technique for the estimation of average reservoir pressure in Naturally Fractured Reservoirs (A.O. Igbokoyi and D. Tiab,2006) is stated as follows:

Step 1. Compute the pressure difference $P_i - P_{wf}(\Delta t)$ for drawdown or

$P_i - P_{wf}(\Delta t)$ for build up or simply ΔP_w ,and the log derivative $t \times \Delta P'_w$ otherwise

known as $t\dfrac{(\delta \Delta P_w)}{(\delta t)}$ or $\dfrac{(\delta \Delta P_w)}{(\delta \log t)}$

Step 2 Make the log-log plot of ΔP_w , and the log derivative $t \times \Delta P'_w$ versus flowing time for drawdown or Δt for buildup.

Step 3 Identify the unit slope line in the wellbore storage section if available. Compute wellbore storage coefficient using the following equation:

$$C=\frac{qB}{24}\times\left(\frac{t}{\left(\Delta P_w\right)}\right)_{ptw} \tag{3.33}$$

Subscript ptw represents a coordinate on the unit slope line

Step 4. Identify all the characteristic points and lines.

Step 5 Select any value of (txΔPw')r on the 0.5 line (infinite acting radial flow). Compute permeability using Equation 3.15.

$$k=\frac{70.6quB}{\left(h\left(t\times\Delta P'_w\right)_r\right)} \tag{3.34}$$

Step 6 Select any values of $\left(\Delta P_w\right)_r$ and $\left(t\times\Delta P'_w\right)_r$ on the 0.5 line (infinite acting radial flow) at any time t_r within the infinite acting region.Compute the skin factor using equation 16

$$S=\left[\frac{\left(\Delta P_w\right)_r}{\left(t\times\Delta P'_w\right)_r}-\ln\left(\frac{kt_r}{\left(\left(\varphi c_t\right)_{(f+m)}\mu r_w^2\right)}\right)+7.43\right] \tag{3.35}$$

Step 7 Identify the minimum coordinate $\left(t\times\Delta P'_w\right)_{min}$ and t_{min} on the log derivative curve. Compute the storativity ratio using any of the following equations: (3.36),(3.37) or (3.38).

$$\omega=0.15866\left[\frac{\left(t\times\Delta P'_w\right)_{min}}{\left(t\times\Delta P'_w\right)_r}\right]+0.54653\left[\frac{\left(t\times\Delta P'_w\right)_{min}}{\left(t\times\Delta P'_w\right)_r}\right]^2 \tag{3.36}$$

$$\omega=10^{-0.8684}\left[1-\frac{\left(t\times\Delta P'_w\right)_{min}}{\left(t\times\Delta P'_w\right)_r}\right] \tag{3.37}$$

Eq.(3.37) is equivalent to $\omega=10^{-\left(\frac{\delta}{m}\right)}$ where $m=\frac{162.6quB}{kh}=2.303\times\left(t\times\Delta P'_w\right)_r$ (3.37b)

$$\delta P=2\left[\left(t\times\Delta P'\right)_R-\left(t\times\Delta P'\right)_{min}\right] \tag{3.37c}$$

$$\omega=\left[2.9114-\frac{3.5688}{lnN_s}-\frac{6.5452}{N_s}\right]^{-1} \tag{3.38}$$

where $N_s=e^{\left(|-\lambda t|_{Dmin}\right)}$ (3.38b)

and

$$t_{Dmin}=\frac{\left[0.0002637\mathrm{k}_f t_{min}\right]}{\left[\left(\varphi c_t\right)_{(f+m)}\times\mu r_w^2\right]} \tag{3.38c}$$

Step 8. Compute the interporosity flow ratio using any of the Equations (3.39) and (3.40):

$$\lambda=\frac{\left[3792\left(\varphi c_t\right)_{(f+m)}\times\mu r_w^2\right]}{\left(k_f t_m\right)}\left(\omega\ln\left(\frac{1}{\omega}\right)\right) \tag{3.39}$$

$$\lambda=\frac{\left[42.5\left(\varphi c_t\right)_{(f+m)}r_w^2\right]}{qB}\frac{\left(t\times\Delta P'_w\right)_{min}}{t_{min}} \tag{3.40}$$

Step 9 Compute the drainage area using Equation (3.41):

$$A=\frac{\left(0.003318\mathrm{k}_f t_{rsi}\right)}{\left(\left(\varphi c_t\right)_{(f+m)}\mu\right)} \tag{3.41}$$

if the early infinite acting radial flow (fracture flow) and/or late infinite acting radial flow (total system flow) can be identified. If wellbore storage and no flow boundary effects mask the early and late radial flow respectively, and the trough can be identified, then use Equation (3.42):

$$A=\left[\frac{\left(0.003318\mathrm{k}_f t_{minsi}\right)}{\left(\left(\varphi c_t\right)_{(f+m)}\mu\right)}\right]\left[\frac{\left(t\times\Delta P'_w\right)_r}{\left(t\times\Delta P'_w\right)_{min}}\right] \tag{3.42}$$

Where it is possible, use both Equations to compute the area.The results should be very close.

Step 10. Compute the average reservoir pressure using (eq.3.43). Use (eq.3.44) if the condition

$$2\pi t_{DA} \gg \frac{\left(2\pi(1-\omega)^2 r^2\right)_w}{(\lambda A)} \quad \text{is satisfied.}$$

$$\bar{P}(t) = P_i - \left(t \times \Delta P'_w\right)_{pss} - 2\left(t \times \Delta P'_w\right)_r \left[\frac{\left(2\pi(1-\omega)^2 r_w^2\right)}{(\lambda A)}\right] \tag{3.43}$$

$$\bar{P} = P_i - \left(t \times \Delta P'_w\right)_r \left[\frac{\left(t \times \Delta P'_w\right)_{pss}}{\left(\left(\Delta P_w\right)_{pss} - \left(t \times \Delta P'_w\right)_{pss}\right)}\right] \times \left[\ln\left(\frac{2.2458\mathrm{A}}{\left(C_A r_w^2\right)}\right) + 2\mathrm{S}\right] \tag{3.44}$$

3.4 Analysis of a well with an inclined hydraulic fracture in a Naturally Fractured Reservoir

Depending on the nature of the inclined hydraulic fracture (uniform flux or infinite conductivity fracture),the following steps are taken in the analysis of a well in an inclined hydraulic fracture in a naturally fractured reservoir:

Step 1 A plot of well pressure change (ΔP) and pressure derivative (t× $\Delta P'$) values versus test time is made. The presence of a straight line of slope 0.5 (linear flow regime) followed by a horizontal straight line (radial flow regime) indicates that the well is intersected by a uniform flux fracture as shown in Fig 3.4.

For a well intersected by an infinite conductivity fracture, a straight line of slope 0.5 (linear flow regime) followed by the bi-radial flow line of slope 0.36 and a horizontal straight line (pseudo-radial flow regime) is observed as shown in Fig 3.5.

Step 2 - Read the value of $(t\times \Delta P')_{PR}$ corresponding to the infinite acting late-time radial flow line.

Step 3 - Calculate the permeability from Eq 3.6

Step 4 - Obtain the value of $(t\times \Delta P')$ at time t = 1 hr from the linear flow line (extrapolated if necessary), $(t \times \Delta P')_{L1}$. If pressure derivative curve is not well defined, obtain $(\Delta P)_{L1}$.

Step 5 - Calculate the ratio, $\frac{y_f}{\cos\theta_w}$ using (Eq3.14).

If the linear flow line portion of the $(t\times \Delta P')$ is too short or too distorted by near wellbore effect and noise, then $\frac{y_f}{\cos\theta_w}$ should be determined from the half-slope line of ΔP, using (Eq3.15) then use (Eq3.16) to draw the half-slope line of the pressure derivative curve.

Step 6 - Determine the time of intersection of the linear and pseudo-radial flow line from the graph, i.e. t_{LPRi}, using the $(t\times \Delta P')$ curve.

Step 7 - Calculate the ratio $\left(\frac{y_f}{\cos\theta_w}\right)^2 / k$ from (Eq3.17).

Then calculate this ratio using k and $\frac{y_f}{\cos\theta_w}$ values obtained in steps 3 and 5, respectively. If the two ratios are approximately equal, then the values of k and $\frac{y_f}{\cos\theta_w}$ are correct. If these ratios are significantly different, shift one or both straight lines, and repeat steps 2 through 7 until the ratios are equal. Generally, the pressure derivative values during the linear flow regime are more likely to be distorted due to mechanical problems, wellbore storage and skin. Consequently, if the pseudo-radial flow line is well defined, then the linear flow line is probably the one that should be shifted. A shift to the left will decrease the value of $\frac{y_f}{\cos\theta_w}$ and a shift to the right will increase it.

Step 7b – For an inclined uniform flux fracture, continue from **Step 8**, otherwise skip to **Step 19**

Step 8 - if early radial flow regime is observed, read the value of $(t\times \Delta P')_{ER}$ corresponding to the early radial flow line. If early radial flow regime cannot be identified, go to Step 14.

Step 9 - Calculate the inclination angle (θ_w) from Eq. 3.3

Step 10 - Calculate the half fracture length, y_f, from the ratio $\frac{y_f}{\cos\theta_w}$ calculated in step 7 and the angle (θ_w) calculated in step 9.

Step 11 - Determine the time of intersection of the linear and early radial flow line from the graph, i.e. t_{LERi}, using the ($t\times \Delta P'$) curve.

Step 12 - Calculate the half fracture length, y_f, from (Eq3.18)

Compare the newly calculated y_f with the one calculated in Step 10. If the two values are approximately equal, then the y_f values are correct. If these values are significantly different, shift the early radial flow horizontal line, and repeat steps 8 through 12 until the two values are equal. Shifting the early radial flow line up will decrease the value of y_f (i.e. increase $\cos(\theta_w)$ or decrease θ_w) and shifting it down will increase y_f(i.e. decrease $\cos(\theta_w)$ or increase θ_w).

Step 13 –Estimate t_{SPR} by calculating t_{SPR} from Equations (Eq3.19) and (Eq3.20) and taking the maximum value of the two. Skip Steps 14-18 and go on to step 19.

Step 14 – Determine from the graph the starting time of the infinite acting pseudo-radial flow line, t_{SPR}, on the pressure derivative curve.

Step 15 - Calculate the angle (θ_w) from Eq. 3.20

Step 16 - Calculate the half fracture length, y_f, from the ratio $\frac{y_f}{\cos\theta_w}$ calculated in step 7 and angle θ_w calculated in step 15.

Step 17 – Check if y_f and θ_w calculated in step 15 and 16 satisfy the condition of (Eq3.21). If they do, go to Step 19. Otherwise, continue to step 18.

Step 18 – Use t_{SPR} to calculate y_f from Eq.(3.19), and then compute the angle (θ_w) from the ratio $\frac{y_f}{\cos\theta_w}$ calculated in step 7. Then skip to Step 25.

Step 19- For an infinite conductivity fracture,read off the value of $(t\times \Delta P')_{BR1}$ at t = 1 hr.

Step 20- Calculate the ratio $\frac{y_f^{0.72}}{\cos\theta_w}$ from (Eq.: 3.23)

Step 21 – Determine the time of intersection of the bi-radial and pseudo-radial flow line from the graph, i.e. t_{BRPRi}, using the ($t\times \Delta P'$) curve.

Step 22 – Calculate the ratio $\frac{y_f^{0.72}}{\cos\theta_w}$ from (Eq.3.24)

Compare this ratio with the ratio calculated in step 9, if the two ratios are approximately equal, then the value of $\frac{y_f^{0.72}}{\cos\theta_w}$ is correct. If these ratios are significantly different, shift the bi-radial straight lines, and repeat Steps 19 through 22 until the ratios are equal.

Step 23 – Calculate y_f and (θ_w) by combining the ratio $\frac{y_f}{\cos\theta_w}$ calculated in Step 7 with $\frac{y_f^{0.72}}{\cos\theta_w}$ from Step 20.

Step 24 –Estimate t_{SPR} by calculating t_{SPR} from Equations 3.25 and 3.26 and taking the maximum value of the two.

Step 25 - Select any value of (txΔPw')r on the 0.5 line (infinite acting radial flow). Compute permeability using (Eq 3.34).i.e.

$$k=\frac{70.6quB}{\left(h\left(t\times\Delta P'_w\right)_r\right)} \qquad (3.34)$$

Step 26-Identify the minimum coordinate $\left(t\times\Delta P'_w\right)_{min}$ and t_{min} on the log derivative curve. Compute the storativity ratio (ω) using any of the following equations: (3.36),(3.37) or (3.38).

Step 27- Compute the interporosity flow ratio using any of the Equations (3.39) and (3.40).

Step 28-Compute the average reservoir pressure using (eq.3.43). Use (eq.3.44) if the condition $2\pi t_{DA} \gg \frac{\left(2\pi(1-\omega)^2 r^2\right)_w}{(\lambda A)}$ is satisfied.

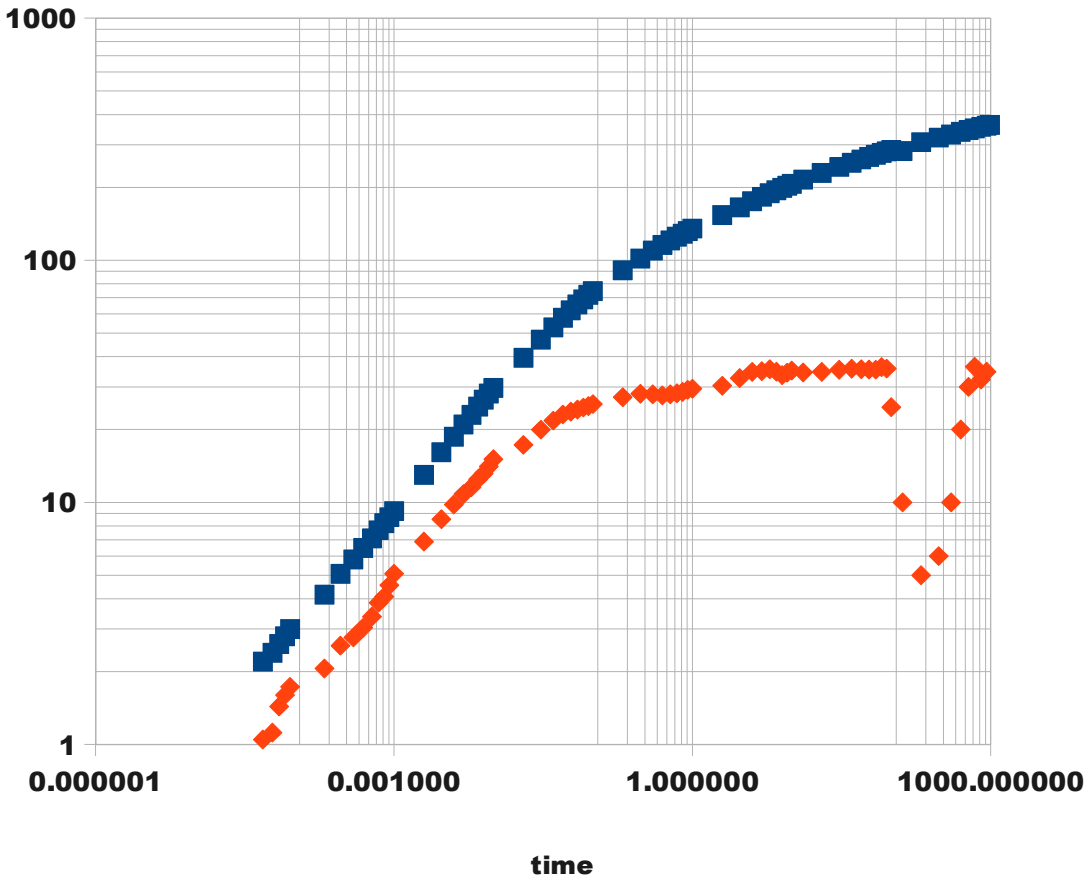

Fig 3.4 P & t*P' plots of a well with an inclined hydraulic fracture (infinite conductivity) in a NFR

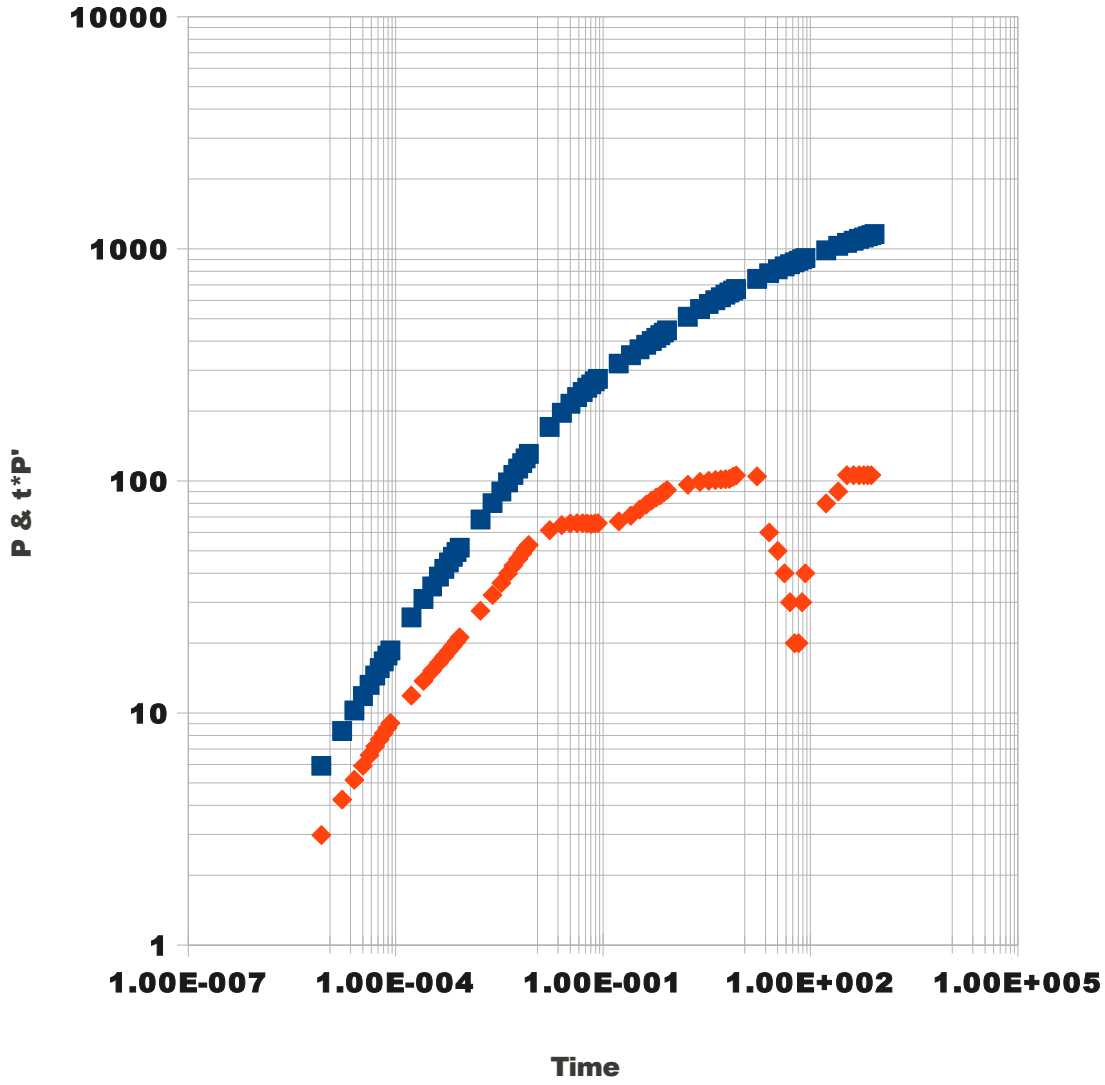

Fig 3.5 P & t*P' plots of a well with an inclined hydraulic fracture (uniform flux) in a NFR

Examples:

CHAPTER 4

CONCLUSIONS

- A technique based on the pressure derivative concept for interpreting pressure transient tests in wells with an inclined hydraulic fracture in a naturally fractured reservoir has been developed.
- The technique (known as the TDS) developed provides an accurate approach which does not involve the use of any chart.
- TDS technique is a practical technique to analyzed inclined fracture pressure data,especially when the data do not match any type curve.The fact that TDS technique only uses log-log plot of pressure & pressure derivative makes it a convenient technique to use.

CHAPTER 5

RECOMMENDATIONS

1 Efforts should be made to program this newly developed procedures in a user-friendly computer language

2 This study can be extended to include finite conductivity inclined fracture in a Naturally Fractured Reservoir.

3 Study can be extended to cases in which the fracture is asymmetric.

Nomenclature

Δt Shut-in time difference, hr

B oil volumetric factor, rb/STB

c_t compressibility, 1/psi

h formation thickness, ft

h_w fracture height, ft

k Formation permeability, md

m_{BR} slope of bi-radial flow line, psi/$hr^{0.36}$

m_{ER} slope of early radial flow line, psi/hr

m_{LF} slope of linear flow line, psi/$hr^{1/2}$

m_{PR} slope of pseudo radial flow line, psi/hr

P pressure, psi

P' pressure derivative, psi/hr

P'_D dimensionless pressure derivative

P_D dimensionless pressure

P_{fD} dimensionless fracture pressure

P_i initial pressure, psi

P_{wf} flowing well pressure, psi

P_{ws} shut-in well pressure, psi

q, q_w oil/well flow rate, BPD

r radial distance ft

r_w wellbore radius, ft

S pseudo-skin factor

t time, hr

t_D dimensionless time

t_{DSPR} Dimensionless time reflecting the start of pseudo-radial flow line

t_p producing time, hr

x x coordinate

y y coordinate

y_f fracture half length, ft

z z coordinate

z_w z coordinate of the fracture and well intersection, ft

Greek symbols

Δ change, drop

ϕ Porosity

μ viscosity, cp

ΔP pressure difference, psi

$\Delta P'$ Change of rate of pressure with time (pressure derivative), psi

θ inclination angle

θ_w fracture inclination angle with respect to vertical well

τ dummy variable of time

Subscripts

1 time is one hour or dummy variable for maximum t_D

BR bi-radial flow

BRERi intersection of early-radial and bi-radial flow lines

BRPRi intersection of pseudo-radial and bi-radial flow lines

D Dimensionless quantity

ER early radial flow

e equivalent time

f fracture

i Initial conditions or intersection

IC infinite conductivity

L linear flow

LBRi intersection of linear and bi-radial flow lines

LERi intersection of linear and early radial flow lines

LF linear flow

LPRi intersection of pseudo-radial and linear flow lines

m correspond to point M in space or slope of the line

PR pseudo radial flow

SPR Start of pseudo-radial flow line

t total

UF uniform flux

w Well

wf Flowing condition

ws Shut-in condition

References

Anh V. Dinh, Djebbar Tiab,2009.Transient-Pressure Analysis of a Well with an Inclined Hydraulic Fracture Using Tiab's Direct Synthesis Technique.Paper SPE 120545 presented at the 2009 SPE Production and Operations Symposium, Oklahoma City, Oklahoma, USA, 4–8 April 2009.

A.O. Igbokoyi and D. Tiab, SPE, U. of Oklahoma,Estimation of Average Reservoir Pressure and Drainage Area in Naturally Fractured Reservoirs—Tiab's Direct Synthesis

Cinco-Ley, H., Ramey,H. J. and Miller, F. G. 1975. Unsteady-State Pressure Distribution Created by a Well with an Inclined Fracture. Paper SPE 5591 presented at the 50th SPE Annual Fall Meeting, Dallas, TX.

Cinco-Ley, H. 1974. Unsteady-State Pressure Distribution Created by a Slanted Well or a Well with an Inclined Fracture. PhD dissertation, Stanford U., Stanford, CA.

Cipolla, C. L. and Wright, C. A. 2000. Diagnostic Techniques to Understand Hydraulic Fracturing: What? Why? And How? Paper SPE 59735 presented at the SPE/CERI Gas Technology Symposium, Calgary, Alberta, Canada, 3-5 April.

Cipolla, C. L. and Wright, C. A. 2000. State-of-the-Art in Hydraulic Fracture Diagnostics. Paper SPE 64434 presented at the SPE Asia pacific Oil and Gas Conference and Exhibition, Brisbane, Australia, 16-18 Oct.

Daneshy, A. A. 1972. A Study of Inclined Hydraulic Fractures. Paper SPE 4062 presented at the 47th Annual Fall Meeting, San Antonio, TX, 8-11 Oct..

Daneshy, A. A. 1970. True and Apparent Direction of Hydraulic Fractures. Paper SPE 3226 presented at the Fifth Conference on Drilling and Rock Mechanics, Austin, TX, 5-6 Jan.

Dunlap, I. R. 1962. Factors Controlling the Orientation and Direction of Hydraulic Fractures. Paper SPE 468 available from SPE online library.

Gringarten, A. C., Ramey, H. J., Jr., and Raghavan, R. 1974. Unsteady-State Pressure Distributions Created by a Well With a Single Infinite-Conductivity Vertical Fracture. *SPEJ* (Aug. 1974): 347-360.

Howard, G. C. and Fast, C. R. 1970. *Hydraulic Fracturing*. Monograph Vol. 2 of the Henry L. Doherty series, SPE of AIME, Dallas, TX.

Hubbert, M. King and Willis, G. David. 1957. Mechanics of Hydraulic Fracturing. *Trans.*, AIME **210**: 153-168.

Minner, W. A., Wright, C. A., Stanley G. R., de Pater, C. J., Gorham, T. L., Eckerfield, L. D. and Hejl, K. A. 2002. Waterflood and Production Induced Stress Changes Dramatically Affect Hydraulic Fracture Behavior in Lost Hills Infill Wells. Paper SPE 77536 presented at the SPE Annual Technical Conference and Exhibition, San Antonio, TX, 29 Sep.- 2 Oct.

Tiab, D. 2005. Analysis of Pressure Derivative Data of Hydraulic Fractured Wells by the Tiab's Direct Synthesis Technique. *Journal of Petroleum Science and Engineering* **49**: 1-21.

Tiab, D. 1994. Analysis of Pressure Derivative without Type-Curve Matching: Vertically Fractured Wells in Closed Systems. *Journal of Petroleum Science and Engineering* **11**: 323-333. This paper was originally presented as SPE 26138 at the 1993 SPE Western Regional Meeting, held in May 26-28, Anchorage, Alaska.

Wright, C. A. and Conant, R. A. 1995. Hydraulic Fracture Reorientation in Primary and Secondary Recovery from Low Permeability Reservoirs. Paper SPE 30484 presented at the SPE Annual Technical Conference, Dallas, TX, 22-25 Oct.

Wright, C. A., Davis, Minner, W. A.,E. J., Ward, J. F., and Weijers, L. 1998. Surface Tiltmeter Fracture Mapping Reaches New Depths – 10000 Feet, and Beyond? Paper SPE 39919 presented at the SPE Rocky Mountain Regional/Low-Permeability Reservoir Symposium and Exhibition, Denver, Colorado, 5-8 April.

Wright, C. A., Stewart, D. A., Emanuele, M. A., and Wright, W. W. 1994. Reorientation of Propped Refracture Treatments in the Lost Hills Field. Paper SPE 27896 presented at the SPE Western Regional Meeting, Long Beach, CA, March 23-25.

SI Metric Conversion Factors

bbl x $1.589873 \times 10^{-1} = m^3$

ft x 3.048×10^{-1}* = m

ft^3 x 2.831685×10^{-2} = m^3

bar x $1.0 \times 10^{+5}$ = Pa

psi x 6.894 757 = kPa

°F (°F − 32)/1.8 = °C

*Conversion factor is exact

Appendix B Definitions of dimensionless terms

$$x_D = \frac{x_m}{y_f} \quad \text{.....(A.1)}$$

$$y_D = \frac{y_m}{y_f} \quad \text{.....(A.2)}$$

$$z_D = \frac{z_m}{y_f} \quad \text{.....(A.3)}$$

$$h_{wD} = \frac{h_w}{y_f} \quad \text{.....(A.4)}$$

$$z_{wD} = \frac{z_w}{y_f} \quad \text{.....(A.5)}$$

$$h_D = \frac{h}{y_f} \quad \text{.....(A.6)}$$

$$t_D = \frac{0.0002637\ kt}{\varphi\ \mu\ c_t\ y_f^2} \quad \text{.....(A.7)}$$

$$P_D(x_D, y_D, z_D, t_D, \theta_w, z_{wD}, h_{wD}, h_D) = \frac{kh\ \Delta P(x_m, y_m, z_m, t, \theta_w, z_w, h_w, y_f, h)}{141.2q\ \mu\ B} \quad \text{.....(A.8)}$$

Where x_m, x_m, x_m,y_f, h_w, z_w, h are in feet, t is in hours, q is in STB/day, B is in rbbl/STB, μ is in cp, and ΔP is in psi. ΔP is equal to $P_i - P_{wf}$ for drawdown tests and $P_{ws} - P_{wf\,(\Delta t=0)}$ for buildup tests.

Appendix B: Data for Fig 3.4 and 3.5:

Data for Fig 3.4:

Dt(hrs)	DP(psi)	DP' (psi/hr)	t*DP'(psia)
0.000000	0		
0.000048	2.2	21833.33	1.05
0.000060	2.39	18651.52	1.12
0.000070	2.6	20500.00	1.44
0.000080	2.8	20000.00	1.60
0.000090	3	19212.12	1.73
0.000200	4.16	10306.57	2.06
0.000290	5.07	8826.90	2.56
0.000390	5.81	7100.00	2.77
0.000490	6.49	6202.60	3.04
0.000600	7.1	5626.41	3.38
0.000700	7.67	5500.00	3.85
0.000800	8.2	5100.00	4.08
0.000900	8.69	5050.00	4.55
0.001000	9.21	5071.82	5.07
0.002000	13	3445.00	6.89
0.003000	16.1	2840.00	8.52
0.004000	18.68	2450.00	9.80
0.005000	21	2165.00	10.83
0.006000	23.01	1925.00	11.55
0.007000	24.85	1780.00	12.46
0.008000	26.57	1645.00	13.16
0.009000	28.14	1565.00	14.09
0.010000	29.7	1507.82	15.08
0.020000	39.56	864.00	17.28
0.030000	46.98	665.50	19.97
0.040000	52.87	544.00	21.76
0.050000	57.86	461.50	23.08
0.060000	62.1	394.50	23.67
0.070000	65.75	345.00	24.15
0.080000	69	308.00	24.64
0.090000	71.91	277.50	24.98
0.100000	74.55	254.84	25.48
0.200000	90.87	135.90	27.18
0.300000	101.73	93.65	28.10
0.400000	109.6	69.85	27.94
0.500000	115.7	55.35	27.68
0.600000	120.67	46.55	27.93
0.700000	125.01	40.30	28.21
0.800000	128.73	35.70	28.56
0.900000	132.15	32.40	29.16
1.000000	135.21	29.49	29.49
2.000000	153.55	15.17	30.33
3.000000	165.54	10.87	32.61
4.000000	175.29	8.65	34.58
5.000000	182.83	6.97	34.83
6.000000	189.22	5.91	35.49
7.000000	194.66	4.95	34.65
8.000000	199.12	4.20	33.56
9.000000	203.05	3.82	34.34
10.000000	206.75	3.51	35.07
13.000000	215.53	2.65	34.41
20.000000	229.49	1.73	34.58
30.000000	242.99	1.18	35.31
40.000000	253.03	0.89	35.68
50.000000	260.83	0.71	35.50
60.000000	267.23	0.59	35.37
70.000000	272.62	0.50	35.35
80.000000	277.33	0.45	36.20
90.000000	281.67	0.40	35.69
100.000000	285.26	0.25	24.74
130.000000	282.6408269	0.05	10.00
200.000000	307.67	0.27	5.00
300.000000	321.11	0.12	6.00

Data for Fig 3.5

Time	Pwf	dPwf	t*dP'wf
8.42E-006	5194.1	5.925	2.98
1.68E-005	5191.6	8.379	4.236
2.53E-005	5189.7	10.262	5.151
3.37E-005	5188.2	11.847	5.922
4.21E-005	5186.8	13.24	6.591
5.05E-005	5185.5	14.494	7.18
5.89E-005	5184.4	15.64	7.706
6.74E-005	5183.3	16.7	8.18
7.58E-005	5182.3	17.689	8.634
8.42E-005	5181.4	18.621	9.054
1.68E-004	5174.2	25.827	11.896
2.53E-004	5169	31.006	13.759
3.37E-004	5164.8	35.165	15.224
4.21E-004	5161.3	38.695	16.464
5.05E-004	5158.2	41.793	17.557
5.89E-004	5155.4	44.573	18.544
6.74E-004	5152.9	47.108	19.451
7.58E-004	5150.6	49.448	20.344
8.42E-004	5148.4	51.636	21.206
1.68E-003	5131.7	68.306	27.57
2.53E-003	5119.7	80.32	32.255
3.37E-003	5109.9	90.135	36.337
4.21E-003	5101.4	98.627	39.978
5.05E-003	5093.8	106.202	43.203
5.89E-003	5086.9	113.078	46.03
6.74E-003	5080.6	119.389	48.489
7.58E-003	5074.8	125.228	51.003
8.42E-003	5069.3	130.736	52.999
1.68E-002	5029.3	170.728	61.356
2.53E-002	5003.5	196.474	64.513
3.37E-002	4984.8	215.24	65.52
4.21E-002	4970.1	229.91	65.765
5.05E-002	4958.1	241.904	65.705
5.89E-002	4948	252.022	65.518
6.74E-002	4939.2	260.757	65.29
7.58E-002	4931.6	268.434	65.601
8.42E-002	4924.6	275.386	65.846
1.68E-001	4879.6	320.427	66.928
2.53E-001	4852	348.026	70.858
3.37E-001	4831	368.98	75.291
4.21E-001	4813.8	386.205	79.147
5.05E-001	4799.1	400.926	82.271
5.89E-001	4786.2	413.808	84.772
6.74E-001	4774.7	425.267	86.793
7.58E-001	4764.4	435.591	89.458
8.42E-001	4754.8	445.187	91.411
1.68E+000	4689.9	510.086	96.373
2.53E+000	4650.2	549.813	98.997
3.37E+000	4621.5	578.5	100.233
4.21E+000	4599	600.955	100.933
5.05E+000	4580.6	619.402	101.378
5.89E+000	4564.9	635.056	101.685
6.74E+000	4551.3	648.65	101.907
7.58E+000	4539.3	660.664	104.146
8.42E+000	4528.2	671.839	105.632
1.68E+001	4456.9	743.069	104.742
2.53E+001	4414	786.007	60
3.37E+001	4383.5	816.473	50
4.21E+001	4359.9	840.104	40
5.05E+001	4340.6	859.412	30
5.89E+001	4324.3	875.736	20